SSRG International Journal of Electrical and Electronics Engineering
ISSN: 2348-8379 / https://doi.org/10.14445/23488379/IJEEE-V10I2P102

Volume 10 Issue 2, 8-18, February 2023
© 2023 Seventh Sense Research Group®

Original Article

Modelling and Analysis of Hybrid Fuzzy Tuned PI Controller based PMBLDC Motor for Electric Vehicle Applications

K.S. Kavin[1], P. Subha Karuvelam[2], Abhinav Pathak[3], T.R Premila[4], R. Hemalatha[5], Tharwin Kumar[6]

[1, 2]Department of Electrical and Electronics Engineering, Government College of Engineering, Tirunelveli, Tamilnadu, India.
[3]Department of Electrical Engineering, Medi-Caps University, Indore.
[4]Department of Electrical and Electronics Engineering, Vels Institute of Science Technology and Advanced Studies, Chennai.
[5]Department of Electrical and Electronics Engineering, Saveetha Engineering College, Tamilnadu, India.
[6] Department of Electrical and Electronics Engineering, Puducherry Technological University, Puducherry, India.

[1]Corresponding Author: kavinksk@gmail.com.

Received: 20 December 2022 Revised: 03 February 2023 Accepted: 12 February 2023 Published: 28 February 2023

Abstract *- Permanent magnet machines are very suitable for Electric vehicles and Motor pump applications because of their simple construction, ease of control and high efficiency. Among the different Permanent Magnet Brushless DC motors (PMBLDC) as well as permanent magnet motors are particularly very suitable for EV applications owing to their high-speed performance and constant speed-torque features. In this paper, the PMBLDC motor is modelled and analysed mathematically using its equivalent circuit. The PMBLDC motor speed is controlled using an intelligent fuzzy logic-tuned PI controller. This fuzzy logic-tuned PI controller and hysteresis current controller (HCC) perform steady state speed and closed loop speed control operation. This proposed hybrid speed controller reduces the second-order underdamped system drawbacks such as settling time, integral absolute error, steady-state error and maximum peak overshoot. A proposed controller achieves a settling time for motor speed at 0.1 s, which provides smooth control for the speed of the PMBLDC motor. The design and modelling of the entire work are done with Matlab's help to verify the proposed hybrid system's performance.*

Keywords *- PMBLD0C motor, Hybrid fuzzy tuned PI controller, PMSM motor, Electronic commutator, Integral error.*

1. Introduction

Though widely used at present, conventional fuel-based vehicles have their drawbacks, such as pollution, high fuel cost, low power efficiency and limited speed range [1]. In order to overcome the drawbacks associated with conventional fuel-based vehicles, there emerges a need to move to Electric vehicles [2][3][4]. Electric vehicles generally use different types of motors, such as DC Shunt, Series and three phases Induction motors (IM). However, these motors have disadvantages like the restricted range of speed, utilising high input power and heavy winding losses. Permanent magnet-based motors reduce the above disadvantages of conventional Electric motors. Permanent Magnet Synchronous Motors (PMSM) and Permanent Magnet Asynchronous Motors are two types of permanent magnet motors. A control circuit of a PMSM is complex when compared to an Asynchronous motor. The best known Permanent magnet Asynchronous motor is the PMBLDC motor [5]. This motor possesses huge merits compared to other motors, such as less Power consumption, high operating Speed range, high efficiency, ease of control, high power density and torque to inertia ratio. These merits give the PMBLDC motor an edge over other motors and make it more suitable for Electric vehicle applications [5].

Though the construction of the PMBLDC motor and the PMSM motor are similar to each other, there is a difference in the rotor construction. PMSM uses a Smooth cylindrical typed rotor, whereas a PMBLDC motor uses a Salient pole-typed rotor [6]. As the rotor in a PMBLDC motor is made up of a Permanent magnet, the position of the rotor is needed to energise its stator windings, and so a rotor position sensor named a Hall Sensor is used in this motor [7][8]. Three hall sensors are needed to provide exact rotor positions to the BLDC motor controller [9]. Recent research studies have shown the use of back emf detection methods to operate sensorless control of BLDC motor drives [10] [11].

REFERENCES	METHODOLOGY	MERITS	DEMERITS
[21]	Finite Element Analysis	• Lowers losses by changing constructional aspects.	• To perform FEM of motor, cross-section, pole-pitch and number of poles are needed.
[22]	The energy regeneration approach is known as the tow-boost technique for electric vehicles powered by BLDC motors	• Without control over electrical torque, speed changes linearly. • Regenerative braking enhances the amount of energy restored and boosts system performance.	• When using the two-boost method, a second timer is needed to calculate the phase position indices.
[23]	A reliable algorithm for optimising BLDC motor design utilised in the electric oil pump	• The algorithm improves the efficiency of rating, torque ripple and cogging torque.	• In the allotted design period, it is difficult to investigate various motor performance limits easily.
[24]	A BLDC motor drive analytical model with a VSI that uses a neural network to manage hysteresis current	• Neural network controllers are robust to operate systems with parameter changes and provide superior dynamic responsiveness.	• Oscillations and large overshot negatively impact system response if PI gains are not appropriately set.
[25]	Social Ski Driver-optimized speed controller for BLDC motor design	• Achieves quicker time response and improved tracking efficiency.	• BLDC motor flaws lower the motor's efficiency.

But this back emf detection-based sensorless control of the BLDC motor is not suitable for controlling speed below a certain minimum level [12]. To control stator windings, the BLDC motor uses an electronic commutator, a 3Φ Voltage Source Inverter (VSI). In contrast, the conventional DC motor uses a mechanical commutator that increases power loss [13]. A PMBLDC motor's speed is regulated by a closed-loop speed controller, while a BLDC motor's current and torque ripples are minimised by a current controller. [14]. A PI controller is frequently used in closed-loop speed controllers, although it causes concerns with motor speed, such as maximum settling time, peak overshoot and steady state inaccuracy. [15].

Intelligent speed controllers adopting rules and deep learning techniques are used to address these problems [28,29] [16-20]. The increase in the application of load torque, the nature of the current generated by the BLDC and the electronic commutator in the motor cause torque ripples and vibrations problems in the motor [26]. The high-gain continuous conduction DC-DC converters like Boost, SEPIC, CUK, and Luo are used in electronic commutator-fed motors to reduce torque ripple issues caused by commutation. [30].

Research works are advancing the performance of PMBLDC motor-based EV applications using different intelligent and optimised controllers with the support of advanced Photo voltaic system fed high gain DC-DC converters. The proposed work explains the modelling of the BLDC motor with the following different objectives,

- To analyse the BLDC motor based on Motor equivalent circuit for EV applications.
- To examine the speed and current controller of the BLDC motor
- To validate performance improvement of PMBLDC motor performance and modelling of BLDC motor curves in Matlab simulation (Matlab 2021a)

The proposed approach is divided into the following sections: motor modelling construction, BLDC motor speed control, simulation research, and closed loop current.

2. Proposed System

The BLDC motor has extensive applications in industrial, commercial, pumping, aerospace and electric vehicles. Figure 1 depicts the proposed block diagram of a closed-loop speed-controlled BLDC motor. An uncontrolled diode bridge rectifier (DBR) feeds the input AC source voltage to 3Φ VSI. It converts AC supply into DC supply. The ripples in the output of the rectifier are suppressed with the smoothening capacitor to get a regulated DC supply. The sequence of rotor positions provided by the hall sensor is used in controlling the BLDC motor. The PWM pulses generated by the controller are given to the electronic commutator.

In order to achieve the closed loop steady speed operation, various speed controllers are used to analyse the speed performance. The second-order underdamped Hybrid PI controller makes efficient steady-state speed operation.

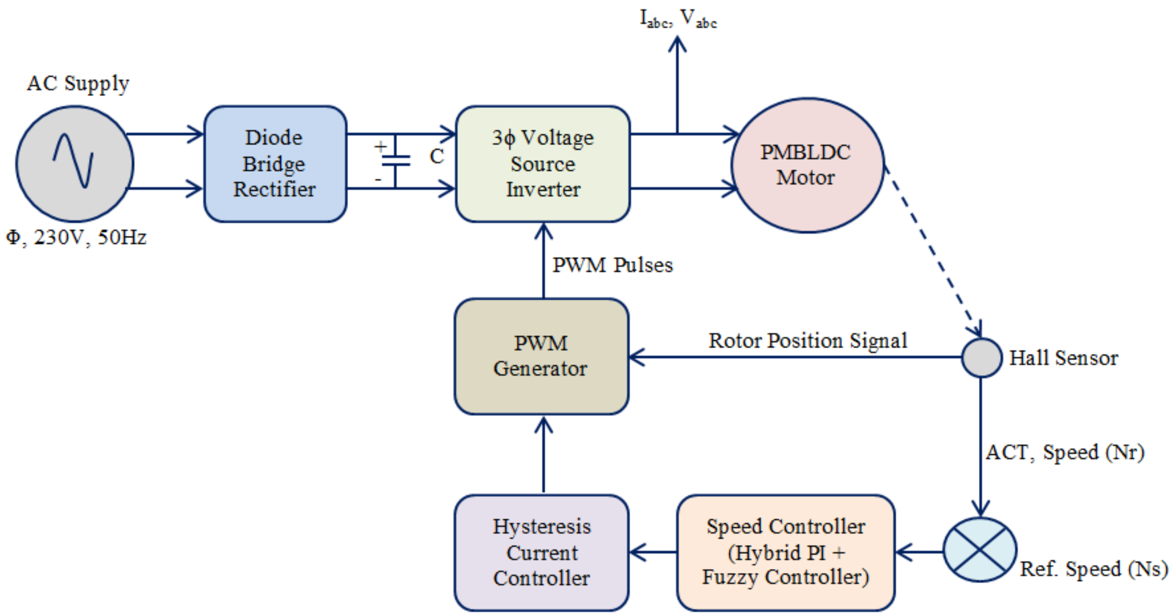

Fig. 1 Proposed work block diagram representation

The difference between the motor's real and reference rotor speeds is controlled using a speed controller, whose output gets transmitted to the current controller using hysteresis. The PWM generator considers the current controller output and hall sensor feedback and produces the sequence of PWM pulses. This PWM pulse sequence is then fed to 3Φ VSI with 60-degree displacement, and finally BLDC motor attains steady state speed operation under varying load conditions.

2.1. BLDC Motor Modelling

A BLDC motor is a trapezoidal-shaped, back emf-based permanent magnet device in which stator winding is energised through 3Φ VSI along with a rotor position signal. The Hall Effect position sensors are mounted in the stator with 120-degree displacement and are used for commutation in the electronic commutator for starting as well as running condition of the BLDC motor. The commutation occurs after each 60-degree revolution of the rotor, depending on the location of the hall sensor. The problems of a conventional DC motor, including Power losses and sparking, are dealt with by an electronic commutator. The voltage source inverter works in two modes: the PWM chopping mode and the freewheeling mode. In these two modes, the duty cycle, the average current, and the average voltage of the motor determine when inverter switches are turned on and off. Figure 2 depicts a circuit that is equivalent to a PMBLDC motor.

BLDC motor is designed with 3Φ stator windings like an Induction motor, and the BLDC rotor is developed using a permanent magnet in the shape of a trapezoid. While considering the mathematical modelling of the BLDC motor, rotor currents are negligible due to the permanent magnet. From the above figure, the equation of voltage of a BLDC motor is drawn and is given below,

$$\begin{bmatrix} v_{as} \\ v_{bs} \\ v_{cs} \end{bmatrix} = \begin{bmatrix} R_s & 0 & 0 \\ 0 & R_s & 0 \\ 0 & 0 & R_s \end{bmatrix} \begin{bmatrix} i_a \\ i_b \\ i_c \end{bmatrix} + \frac{d}{dt} \begin{bmatrix} L_{aa} & L_{ab} & L_{ac} \\ L_{ba} & L_{bb} & L_{bc} \\ L_{ca} & L_{cb} & L_{cc} \end{bmatrix} \begin{bmatrix} i_a \\ i_b \\ i_c \end{bmatrix} + \begin{bmatrix} e_a \\ e_b \\ e_c \end{bmatrix} \quad (1)$$

From equation (1) v_{as}, v_{bs} and v_{cs} indicates voltage applied to the BLDC motor drive from VSI. R_s specifies stator resistance, i_a, i_b and i_c represents the phase current of the stator; L_{aa}, L_{bb} and L_{cc} indicates self-inductance at phases a, b and c; e_a, e_b as well as e_c describes phase back emf. L_{ab}, Land L_{ac} denotes mutual inductances among three phases; Assumptions made for both stator and rotor windings resistance are equal, and the corresponding inductance values are given below,

$$L_{aa} = L_{bb} = L_{cc} = L \quad (2)$$

$$L_{ab} = L_{ba} = L_{ac} = L_{ca} = L_{bc} = L_{cb} = M \quad (3)$$

The detailed model expressions for the BLDC motor are obtained by substituting equations (2) and (3) on equation (1).

$$\begin{bmatrix} v_{as} \\ v_{bs} \\ v_{cs} \end{bmatrix} = \begin{bmatrix} R_s & 0 & 0 \\ 0 & R_s & 0 \\ 0 & 0 & R_s \end{bmatrix} \begin{bmatrix} i_a \\ i_b \\ i_c \end{bmatrix} + \frac{d}{dt} \begin{bmatrix} L & M & M \\ M & L & M \\ M & M & L \end{bmatrix} \begin{bmatrix} i_a \\ i_b \\ i_c \end{bmatrix} + \begin{bmatrix} e_a \\ e_b \\ e_c \end{bmatrix} \quad (4)$$

By using the given equation, voltages are represented by v_{as}, v_{bs} and v_{cs} and written as

$$v_{as} = v_{ao} = v_{no},\ v_{bs} = v_{bo} - v_{no}\ and,\ v_{cs} = v_{co} - v_{no} \quad (5)$$

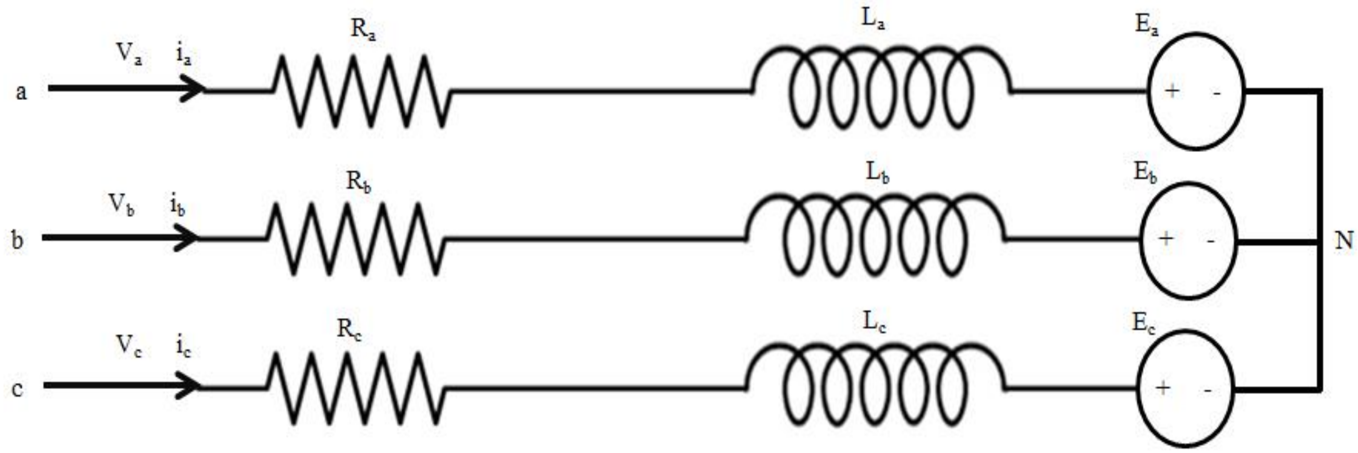

Fig. 2 BLDC motor's equivalent circuit

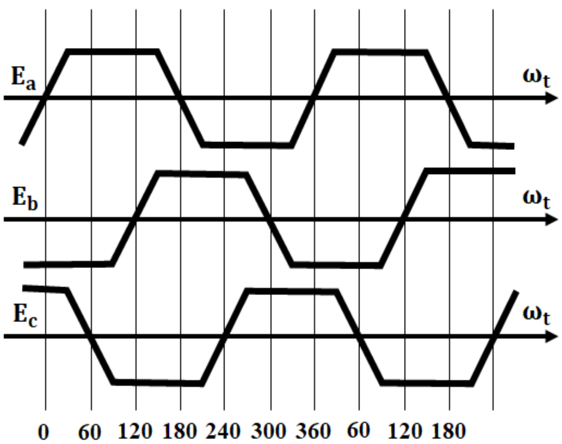

Fig. 3 BLDC motor back emf waveform

Since there are no three-phase neutral voltages, the balanced stator phase currents are fixed. i.e.

$$i_a = i_b = i_c = 0 \tag{6}$$

With the above conditions, the inductances matrix is simplified as

$$Mi_b + Mi_c = -Mi_a \tag{7}$$

The below equation provides BLDC motor modelling in State space form

$$\begin{bmatrix} v_{as} \\ v_{bs} \\ v_{cs} \end{bmatrix} = \begin{bmatrix} R_s & 0 & 0 \\ 0 & R_s & 0 \\ 0 & 0 & R_s \end{bmatrix} \begin{bmatrix} i_a \\ i_b \\ i_c \end{bmatrix} + \frac{d}{dt} \begin{bmatrix} L-M & M & M \\ M & L-M & M \\ M & M & L-M \end{bmatrix} \begin{bmatrix} i_a \\ i_b \\ i_c \end{bmatrix} + \begin{bmatrix} e_a \\ e_b \\ e_c \end{bmatrix} \tag{8}$$

The trapezoidal shape of the BLDC motor back emf is given as

$$\begin{bmatrix} e_a \\ e_b \\ e_c \end{bmatrix} = \omega_m \lambda_m \begin{bmatrix} f_{as}(\theta_r) \\ f_{bs}(\theta_r) \\ f_{cs}(\theta_r) \end{bmatrix} \tag{9}$$

From equation (9), the angular rotor speed is denoted as ω_m, flux linkage as λ_m, the position of the rotor as θ_r and $f_{as}(\Theta_r)$, $f_{bs}(\Theta_r)$ and $f_{cs}(\Theta_r)$ are the functions. The following Figure 3 depicts the back emf waveform of the PMBLDC motor in a trapezoidal shape.

The electromagnetic torque is defined from the above back emf equation

$$T_e = [e_a i_a + e_b i_b + e_c i_c]/\omega_c(N-m) \tag{10}$$

The moment of inertia of the BLDC motor is determined by

$$J = J_m + J_l \tag{11}$$

Load torque is

$$\frac{d\omega_m}{dt} + B\omega_m = (T_e - T_l) \tag{12}$$

The position of the BLDC motor is

$$\frac{d\theta_r}{dt} = \frac{p}{2}\omega_m \tag{13}$$

Substituting equation (6) in equation (8) and summing it is given in the form of

$$v_{ao} + v_{bo} + v_{co} - 3v_{no} = (i_a + i_b + i_c)R_s + (pi_a + pi_b + p_{ic})(L-M) + (e_a + e_b + e_c) \tag{14}$$

Applying equation (6) to equation (14) will provide the following equation:

$$v_{ao} + v_{bo} + v_{co} - 3v_{no} = (e_a + e_b + e_c)$$

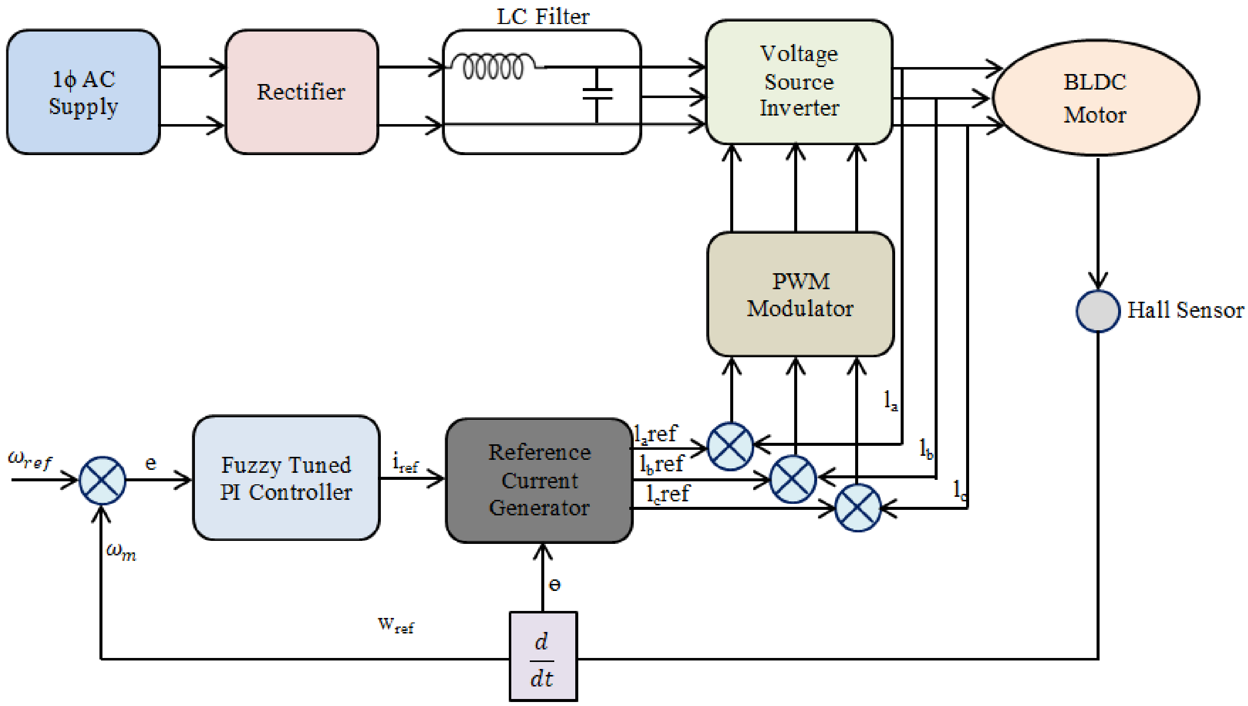

Fig. 4 Block representation of fuzzy-PI controller for BLDC drive

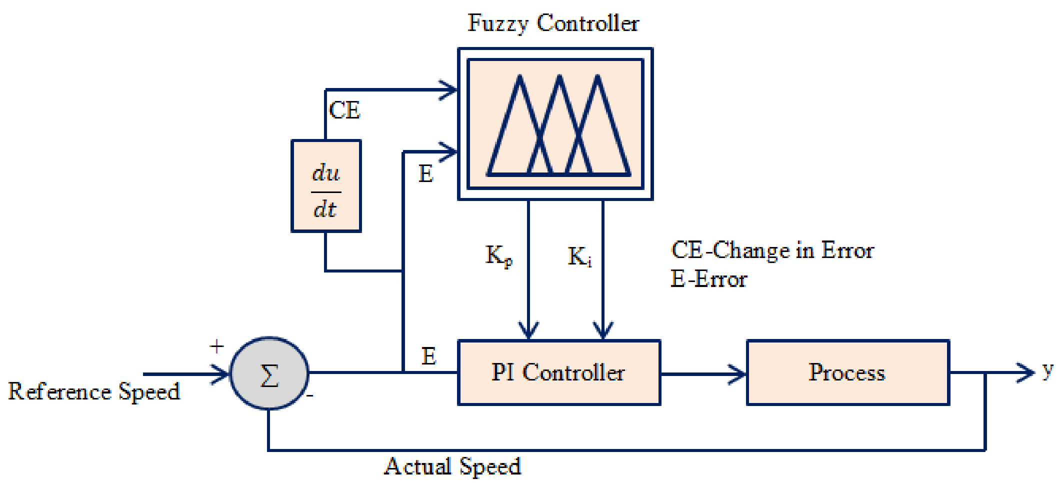

Fig. 5 Fuzzy-PI speed control of motor

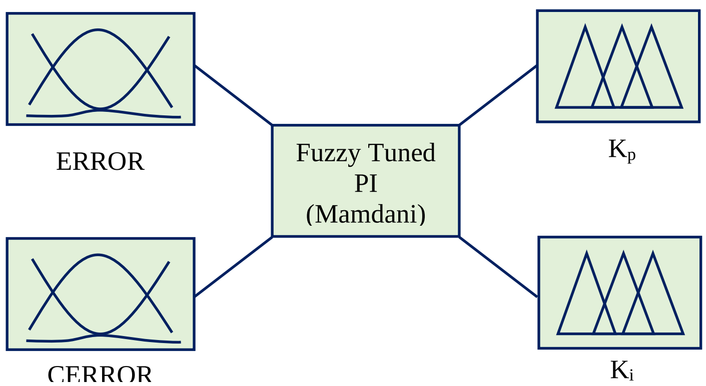

Fig. 6 Membership type of FLC

Hence,

$$v_{no} = [v_{ao} + v_{bo} + v_{co}] - (e_a + e_b + e_c)]/3 \quad (15)$$

When equations are combined,

$$\dot{x} = A_x + B_u + C_e \quad (16)$$

Here

$$x = [i_a \quad i_b \quad i_c \quad \omega_m \quad \theta_r]^t \quad (17)$$

$$A = \begin{bmatrix} -\frac{R_s}{L-M} & 0 & 0 & -\frac{\lambda_m}{J} f_{as}(\theta_r) & 0 \\ 0 & -\frac{R_s}{L-M} & 0 & -\frac{\lambda_m}{J} f_{bs}(\theta_r) & 0 \\ 0 & 0 & -\frac{R_s}{L-M} & -\frac{\lambda_m}{J} f_{cs}(\theta_r) & 0 \\ \frac{\lambda_m}{J} f_{as}(\theta_r) & \frac{\lambda_m}{J} f_{bs}(\theta_r) & \frac{\lambda_m}{J} f_{cs}(\theta_r) & -\frac{B}{J} & 0 \\ 0 & 0 & 0 & \frac{P}{2} & 0 \end{bmatrix} \quad (18)$$

$$B = \begin{bmatrix} \frac{1}{L-M} & 0 & 0 & 0 \\ 0 & \frac{1}{L-M} & 0 & 0 \\ 0 & 0 & \frac{1}{L-M} & 0 \\ 0 & 0 & 0 & \frac{1}{L-M} \\ 0 & 0 & 0 & \end{bmatrix}$$

$$B = \begin{bmatrix} \frac{1}{L-M} & 0 & 0 & 0 \\ 0 & \frac{1}{L-M} & 0 & 0 \\ 0 & 0 & \frac{1}{L-M} & 0 \\ 0 & 0 & 0 & \frac{1}{L-M} \\ 0 & 0 & 0 & \end{bmatrix} \quad (19)$$

$$C = \begin{bmatrix} -\frac{1}{L-M} & 0 & 0 \\ 0 & -\frac{1}{L-M} & 0 \\ 0 & 0 & -\frac{1}{L-M} \end{bmatrix} \quad (20)$$

$$u = [v_{as} \quad v_{bs} \quad v_{cs} \quad T_l]^t \quad (21)$$

$$e = [e_a \quad e_b \quad e_c]^t \quad (22)$$

To make the speed of the PMBLDC motor constant, in the following section PI controller is tuned by intelligent FLC.

2.2. Hybrid Fuzzy Tuned PI Controller

An Integral proportional controller considers an appropriate output generated by the inverter that is needed to bring down the value of the error signal to almost zero. Here a steady state speed error is not eliminated completely, but the PI controller gain (K_p) tends to reduce the rise time error. Although an integral control gain (Ki) eliminates steady-state speed error, it worsens the transient response. To determine error speed, the reference and actual output speeds are contrasted. The error speed value is formerly given to the PI speed controller to get the constant speed operation. In the proposed work, the PI controller is tuned using a fuzzy logic algorithm to overcome the existing problems of the PI controller, such as steady-state speed error and transient response. The following Figure 4 depicts the block diagram for the fuzzy-tuned PI controller for the BLDC drive.

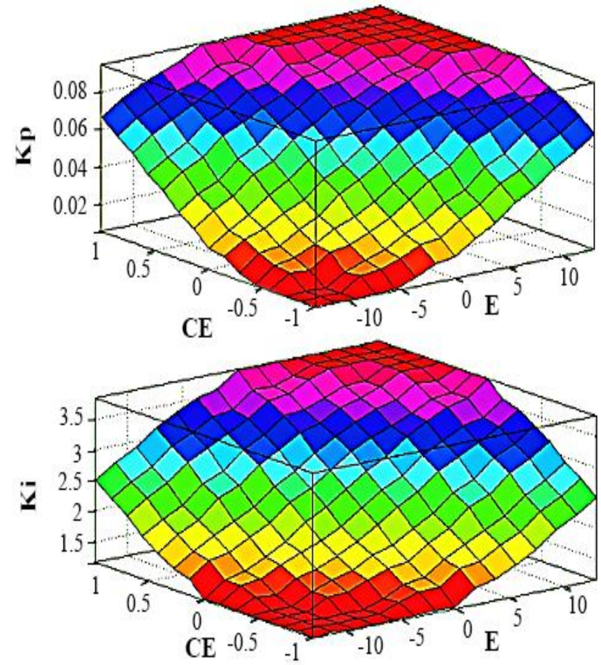

Fig. 7 Surface image for FLC

The objective of self-tuned fuzzy-based PI is to achieve better steady-state speed performance, making it more applicable and suitable to industrial, commercial and EV applications. Figure 5 shows the PI controller adjusted using a fuzzy technique for BLDC motor speed control. PI controller with fuzzy tuning controls the motor's speed, whereas PI controller with adaptive tuning controls the gain.

Figure 6 shows the membership function for the proposed fuzzy controller. The difference in error and motor speed error is input to FLC, and the controller's output is integral gain (K_i) and proportional gain (K_p). This fuzzy controller uses the mamdani type, triangular membership function and 49 rules, which lead to better system performance. Figure 7 shows the surface image for FLC. Following Table 1. shows the fuzzy rules for generating the K_p and K_i values of the PI controller.

The fuzzy-PI controller achieves steady state speed operation with minimised underdamped problems in motor speed waveform. The output signal of the fuzzy-PI controller is supplied to HCC.

2.3. Hysteresis Current Controller

In order to minimise control speed and torque ripple in a closed loop, BLDC motors use HCC. The switches in the voltage source inverter for speed control are examined using control error signal $e(t)$, the variation between reference current $(iref)$ and actual current $(iact)$ of the motor gives error signal $e(t)$. Once the error reaches the maximum limit of the hysteresis band, switches are turned off immediately to make the current as low.

Table 1. FLC rules to tune PI controller gain

CE \ E	NB	NM	NS	ZE	PS	PM	PB
NB	NB	NB	NB	NB	NM	NS	ZE
NM	NB	NB	NB	NM	NS	ZE	PS
NS	NB	NB	NM	NS	ZE	PS	PM
ZE	NB	NM	NS	ZE	PS	PM	PB
PS	NM	NS	ZE	PS	PM	PB	PB
PM	NS	ZE	PS	PM	PB	PB	PB
PB	ZE	PS	PM	PM	PB	PB	PB

Table 2. Specifications of BLDC motor

Number of Poles	4
Power (P)	1 Hp
DC link Voltage (V)	310V
Maximum Torque (T)	1.5 Nm
Maximum speed of the motor (w)	2000RPM
Stator-Inductance (L_ph)	25.71mH
Stator-Resistance (R_ph)	2.8750 ohm
Torque Coefficient Constant (K_t)	0.74 Nm
Input AC voltage Source	230V,5A
Moment of Inertia (J)	1.3e-4kg.m2
Switch used	IGBT

Table 3. Performance parameters of the BLDC motor

Metrics	Method	25% I=2.7 A	50% I=3.1 A	75% I= 3.7 A	100% I=4.2 A
Mp	PI (ZN)	0.021	0.034	0.045	0.056
	FUZZY	0.06	0.062	0.086	0.091
	HYBRID	0.251	0.275	0.289	0.31
Ts	PI (ZN)	0.25	0.26	0.29	0.35
	FUZZY	0.16	0.18	0.23	0.27
	HYBRID	0.042	0.047	0.052	0.059
Ess	PI (ZN)	0.47	0.45	0.48	0.52
	FUZZY	0.3	0.332	0.34	0.36
	HYBRID	0.13	0.17	0.22	0.25
IAE	PI (ZN)	16.8	15.9	15.5	14.1
	FUZZY	9.21	8.76	8.56	8.32
	HYBRID	3.01	3.31	3.56	3.87

Similarly, once when error reaches the minimum limit of the band range, switches are turned on to compensate for compensating current. The conditions for the on and off time of the hysteresis current controller are given below.

Condition for the off state: $(iref - iact) > HB$
Condition for off-state: $(iref - iact) > -HB$

This controller reduces the motor current ripples hugely, and in this work, the hysteresis band limit is assigned as 0.01 with respect to the switching frequency of the inverter switches.

3. Results and Discussion

The entire fuzzy-tuned PI controller-based BLDC motor system is validated using Matlab 2021a version software. The motor is tested under different loading conditions to demonstrate the performance of the PMBLDC motor speed characteristics. The following Table 2 depicts the specification of the PMBLDC motor. Figure 8(a) shows that input AC voltage waveform 230 V is applied to single-phase DBR. A diode bridge rectifier carries out the conversion of the AC voltage waveform into a DC voltage waveform. DBR converts a waveform of AC voltage into DC voltage. The output filter capacitor balances the DBR output voltage. Figure 8(b) depicts the waveform of an AC current that harmonics have suppressed, but this paper does not achieve power factor correction.

Figure 9(a) and 9(b) show the diode bridge rectifier voltage and current waveform. The output voltage from DBR is supplied to 3Φ VSI. The voltage source inverter provides a supply to BLDC motor stator windings, and the PWM pulse to VSI depends on the motor Hall sensor position signal and fuzzy-tuned PI controller output signal.

Figure 10 shows the current waveform BLDC motor with non-linear characteristics and a trapezoidal back emf nature, which makes the BLDC motor current non-sinusoidal. At starting of the BLDC motor, the winding consumes nearly 10 A from the supply, and while running, it is reduced to 1 A. 2 Nm load is applied to the BLDC motor at 1 second. This increases the motor load current to 4.2 A, but the closed loop speed controller makes the motor speed constant while changing the load. Figure 11 illustrates trapezoidal shaped back emf waveform, which affects current and speed waveform. But the closed-loop speed controller and hysteresis current controller control the current and speed of the motor.

The speed waveform is depicted in Figure 12 for the BLDC motor. For the BLDC motor, 2000 rpm is assigned as the reference speed. The proposed speed controller maintains the motor's actual speed at 2000 rpm. Also settling time of the motor is 0.1 s, as seen from the above figure. The following Figure 13 shows the torque waveform of the BLDC motor. Even after varying the load torque, the speed control maintains a constant speed of operation.

Figure 14 shows the speed waveform of the BLDC motor under different reference speeds from 1500 RPM to 2000 RPM. The motor responds quickly as well as maintains a constant speed. Performance characteristics of BLDC motors, including steady-state error, maximum peak overshoot, settling time and integral absolute error at various load current ratings, are shown in Table 3 above. Compared to PI and FLC, this proposed Fuzzy tuned PI controller improves system performance parameters.

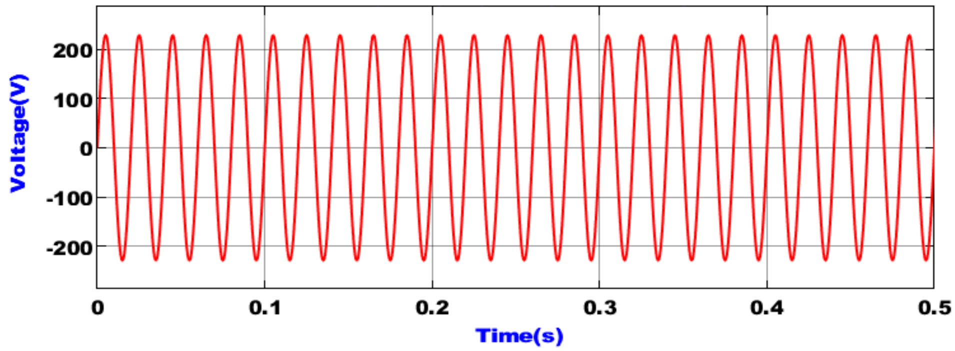

Fig. 8(a) Input voltage waveform

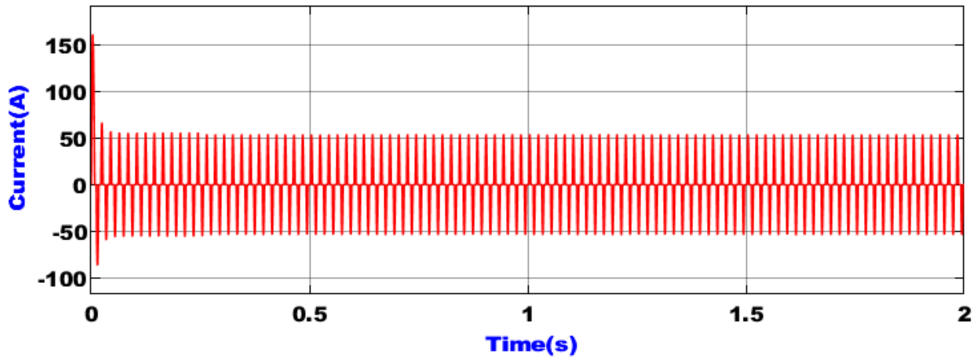

Fig. 8(b) Input current waveform

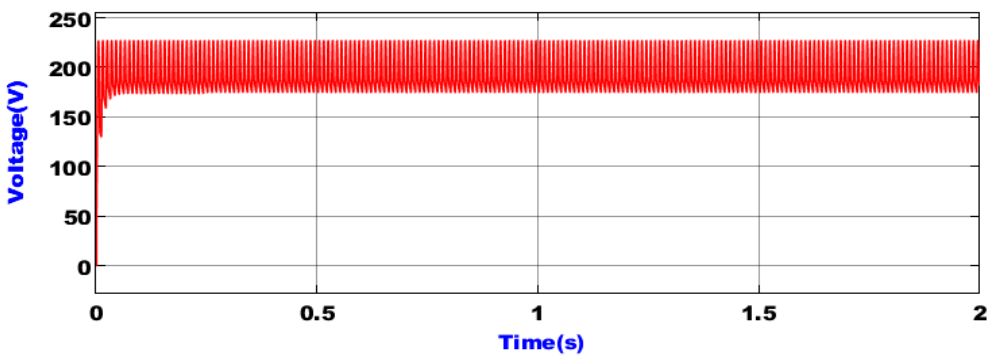

Fig. 9(a) Diode bridge rectifier voltage waveform

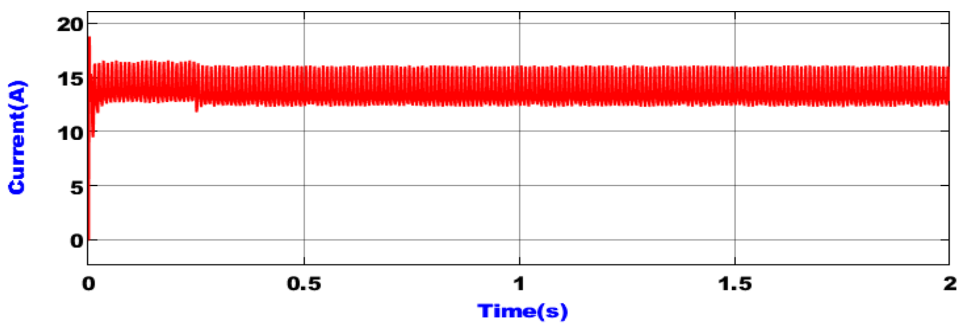

Fig. 9(b) Diode bridge rectifier current waveform

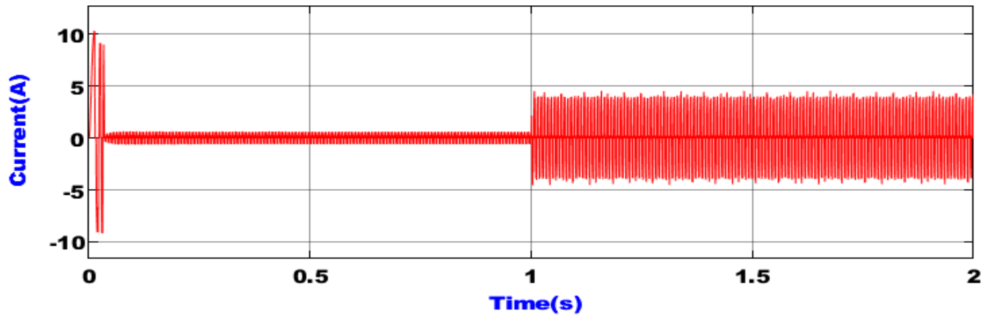

Fig. 10 BLDC motor current waveform

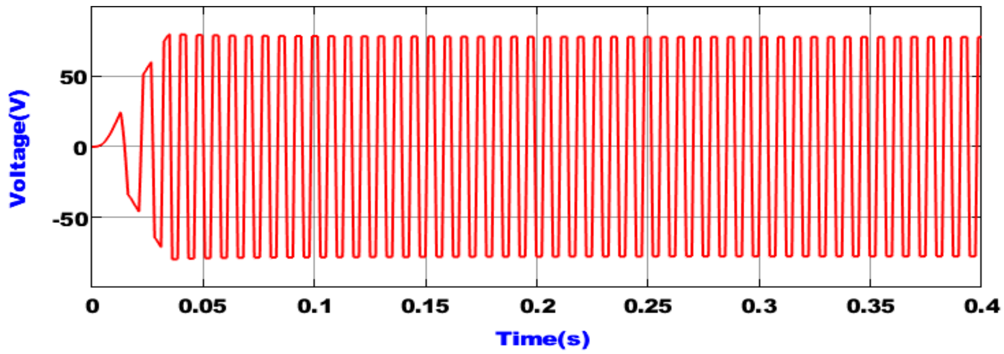

Fig. 11 BLDC motor back emf waveform

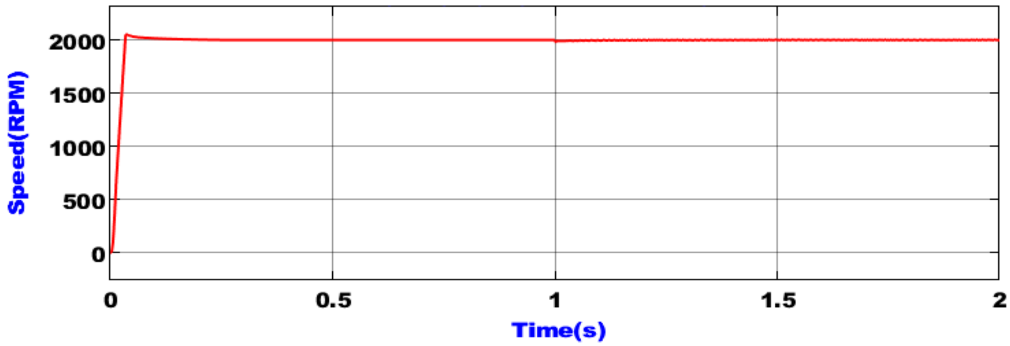

Fig. 12 BLDC motor speed waveform

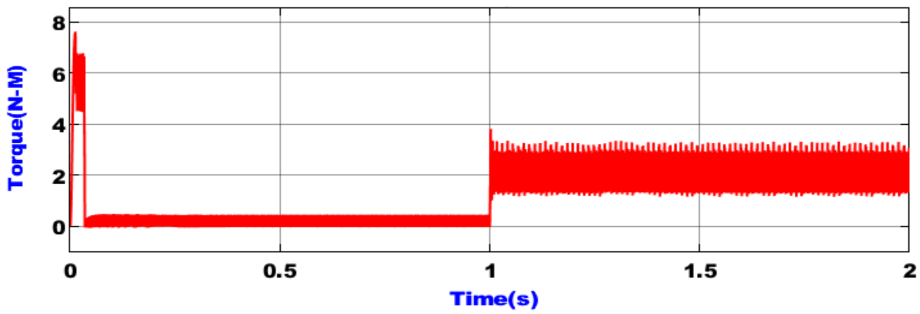

Fig. 13 BLDC motor torque waveform

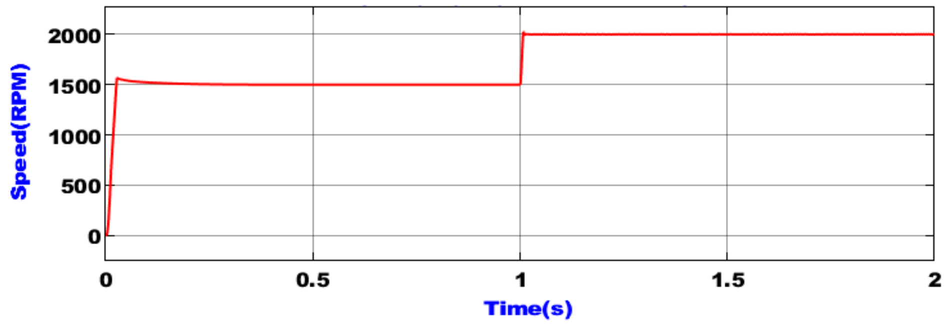

Fig. 14 BLDC motor speed waveform from 1500 rpm to 2000 rpm

4. Conclusion

This paper discusses about the modelling and analysis of the PMBLDC motor with its equivalent circuit. The non-linear current characteristics of the motor increase oscillations in the torque, this torque ripples produce huge oscillations in the speed of the motor. The proposed fuzzy-tuned PI, along with the hysteresis current controller, is used to solve the issue. The proposed speed control maintains constant speed operation with minimised settling time of 0.1s. Also, the BLDC motor was tested with different load ratings, and the results were analysed. The speed control maintains constant speed operation, even after varying the load of the PMBLDC motor. Finally, compared to the existing PI and FLC, this Fuzzy tuned PI controller reduces Integral absolute error, Maximum peak overshoot problem and steady-state error. These advantages make PMBLDC motors more useful for industrial, pumping and EV applications than conventional DC and AC motors.

References

[1] Muhammad Hosnee Mobarak, Rafael N. Kleiman, and Jennifer Bauman, "Solar-Charged Electric Vehicles: A Comprehensive Analysis of Grid, Driver, and Environmental Benefits," *IEEE Transactions on Transportation Electrification*, vol. 7, no. 2, pp. 579-603, 2021. [CrossRef]

[2] Shahab Shamshirband, Timon Rabczuk, and Kwok-Wing Chau, "A Survey of Deep Learning Techniques: Application in Wind and Solar Energy Resources," *IEEE Access*, vol. 7, pp. 164650-164666, 2019. [CrossRef]

[3] Kalpesh Chaudhari et al., "Hybrid Optimization for Economic Deployment of ESS in PV-Integrated EV Charging Stations," *IEEE Transactions on Industrial Informatics*, vol. 14, no. 1, pp. 106-116, 2018. [CrossRef]

[4] Gautham Ram Chandra Mouli et al., "Integrated PV Charging of EV Fleet Based on Energy Prices, V2G, and Offer of Reserves," *IEEE Transactions on Smart Grid*, vol. 10, no. 2, pp. 1313-1325, 2019. [CrossRef]

[5] Prashant Kumar et al., "Iron-Loss Modeling With Sensorless Predictive Control of PMBLDC Motor Drive for Electric Vehicle Application," *IEEE Transactions on Transportation Electrification*, vol. 7, no. 3, pp. 1506-1515, 2021. [CrossRef]

[6] K. S. Kavin, and P. Subha Karuvelam, “PV-based Grid Interactive PMBLDC Electric Vehicle with High Gain Interleaved DC-DC SEPIC Converter,” *IETE Journal of Research*, 2021. [CrossRef]

[7] Poovizhi Mani et al., “An Optimized Design Modelling of PV Integrated SEPIC-Based Four-Switch Inverter for Sensorless PMBLDC Motor Control,” *Automatika*, vol. 63, no. 1, pp. 90-101, 2022. [CrossRef]

[8] Ahmad S. Al-Adsani, Michel E. AlSharidah, and Omid Beik, "BLDC Motor Drives: A Single Hall Sensor Method and a 160° Commutation Strategy," *IEEE Transactions on Energy Conversion*, vol. 36, no. 3, pp. 2025-2035, 2021. [CrossRef]

[9] S. O. Kwon et al., "Loss Distribution of Three-Phase Induction Motor and BLDC Motor According to Core Materials and Operating," *IEEE Transactions on Magnetics*, vol. 45, no. 10, pp. 4740-4743, 2009. [CrossRef]

[10] Haifeng Zhang et al., "High-Precision Sensorless Optimal Commutation Deviation Correction Strategy of BLDC Motor With Asymmetric Back EMF," *IEEE Transactions on Industrial Informatics*, vol. 17, no. 8, pp. 5250-5259, 2021. [CrossRef]

[11] Haifeng Zhang, and Haitao Li, "Fast Commutation Error Compensation Method of Sensorless Control for MSCMG BLDC Motor With Nonideal Back EMF," *IEEE Transactions on Power Electronics*, vol. 36, no. 7, pp. 8044-8054, 2021. [CrossRef]

[12] Jasper De Viaene et al., "Sensorless Load Angle Control for Energy Optimal Sinusoidal Driven BLDC Motor Applications," *IEEE/ASME Transactions on Mechatronics*, vol. 27, no. 4, pp. 2290-2300, 2022. [CrossRef]

[13] Rahat Ullah Khan, "Real Time Performance Evaluation of Modified PMDC Motor, BLDC Motor and Dual Commutator PMDC Machine," *2017 International Conference on Energy, Communication, Data Analytics and Soft Computing*, pp. 2419-2423, 2017. [CrossRef]

[14] Rodolfo L. Valle et al., "Simple and Effective Digital Control of a Variable-Speed Low Inductance BLDC Motor Drive," *IEEE Access*, vol. 8, pp. 13240-13250, 2020. [CrossRef]

[15] Changliang Xia, Zhiqiang Li, and Tingna Shi, "A Control Strategy for Four-Switch Three-Phase Brushless DC Motor Using Single Current Sensor," *IEEE Transactions on Industrial Electronics*, vol. 56, no. 6, pp. 2058-2066, 2009. [CrossRef]

[16] Mohammed. S. Mohammed, Khaled. M. Al-Awasa, and Husssein. D. Al-Majali, "Energy Management and Control in Micro Grid with Hybrid Energy Storage Systems by Using PI and Flatness Theory," *International Journal of Engineering Trends and Technology*, vol. 69, no. 11, pp. 227-235, 2021. [CrossRef]

[17] Ngoc-Khoat Nguyen et al., "Designing an Effective Hybrid Control Strategy to Balance a Practical Inverted Pendulum System," *International Journal of Engineering Trends and Technology*, vol. 70, no. 5, pp. 80-87, 2022. [CrossRef]

[18] Djamel Eddine Beladjine et al., "A Comparative Study of BLDC Motor Speed Control Using PI and ANN Regulator," *2021 18th International Multi-Conference on Systems, Signals & Devices (SSD)*, pp. 1291-1295, 2021. [CrossRef]

[19] Nguyen Thi Thanh Nga, "Design a Hybrid PI – Hedge Algebraic Controller for Controlling Brushless DC Motor," *SSRG International Journal of Electrical and Electronics Engineering*, vol. 5, no. 6, pp. 28-33, 2018. [CrossRef]

[20] R. Karthik Kumar, "Fuzzy Tuned PI Controller for Shunt Active Power Filter," *International Journal of Recent Engineering Science*, vol. 7, no. 6, pp. 23-30, 2020.

[21] Praveenkumar Chandran, Kaliamoorthy Mylsamy, and Prabha Umapathy, "Conceptual Design and Material Analysis of BLDC Motor Using FEA Tools for Electric Vehicle Applications," Technical Journal, vol. 29, no. 3, pp. 1010-1018, 2022. [CrossRef]

[22] Bahrami, Mansour, Hossein Mokhtari, and Amin Dindar, "Energy Regeneration Technique for Electric Vehicles Driven by a Brushless DC Motor," *IET Power Electronics*, vol. 12, no. 13, pp. 3397-3402, 2019. [CrossRef]

[23] Keun-Young Yoon, and Soo-Whang Baek, "Robust Design Optimization with Penalty Function for Electric Oil Pumps with BLDC Motors," *Energies*, vol. 12, no. 1, p. 153, 2019. [CrossRef]

[24] Senthil Kumar R, I. Gerald Christopher Raj, and S. Sharavanan, "Performance Analysis of BLDC Motor Drive using Enhanced Neural Based Speed Controller for Electric Vehicle Applications," *International Journal of Vehicle Structures and Systems*, vol. 12, no. 2, pp. 235-240, 2020. [CrossRef]

[25] Arun Eldho Alias, and F. T. Josh, "Design Analysis of SSD Optimized Speed Controller for BLDC Motor," *International Journal of Electrical and Electronics Research*, vol. 10, no. 3, pp. 529-535, 2022. [CrossRef]

[26] Harshwardhan Soni, and V.G. Durgarao Rayudu, "ANFIS-Controlled Voltage Source for Vigorous Speed Control of BLDC Motor Drive for Utilization in Smart Electric Vehicles," *2022 2nd International Conference on Emerging Frontiers in Electrical and Electronic Technologies*, pp. 1-6, 2022. [CrossRef]

[27] Mr. Satish B. Tarpe, and Dr. Ram S. Dhekekar, "Review: Real Time Implementation of FPGA Base System - Speed Control of DC Motor using PID Controller," *SSRG International Journal of Electronics and Communication Engineering*, vol. 2, no. 3, pp. 20-23, 2015. [CrossRef]

[28] Bo-pi Jin et al., "High Precision Servo Control of Single-phase BLDC motor based on Fuzzy self-tuning PID," *2022 International Symposium on Control Engineering and Robotics (ISCER)*, pp. 38-41, 2022. [CrossRef]

[29] Manish S. Trivedi, and Ritesh Kumar Keshri, "Evaluation of Predictive Current Control Techniques for PM BLDC Motor in Stationary Plane," *IEEE Access*, vol. 8, pp. 46217-46228, 2020. [CrossRef]

[30] K. Balamurugan et al., "Comparative Analysis of CUK, SEPIC, Buck-Boost and ZETA Converters to Reduce Commutation Torque Ripple in BLDC Motor," *2022 International Conference on Advanced Computing Technologies and Applications (ICACTA)*, pp. 1-7, 2022. [CrossRef]

[31] Dr. G. Dinesh, "A Modified Self Tuning Fuzzy Logic Controller for Brushless Direct Current Motor," *International Journal of Recent Engineering Science*, vol. 1, no. 4, pp. 22-27, 2014.